

# Odd and Even Model Self-Assembled Monolayers: Links between Friction and Structure

Paul T. Mikulski,<sup>\*,†</sup> Lawrence A. Herman,<sup>§</sup> and Judith A. Harrison<sup>\*,‡</sup>

*Departments of Physics and Chemistry, United States Naval Academy,  
Annapolis, Maryland 21402*

*Received July 27, 2005. In Final Form: September 30, 2005*

The friction between an amorphous carbon tip and two *n*-alkane monolayers has been examined using classical molecular dynamics simulations. The two monolayers have the same packing density, but the chains comprising each monolayer differ in length by one  $-\text{CH}_2-$  unit. The simulations show that the monolayers composed of  $\text{C}_{13}$  chains have higher friction than those composed of  $\text{C}_{14}$  chains when sliding in the direction of chain cant; the difference in friction becomes more pronounced as the load is increased. Examination of the contact forces between the chains and the tip, along with conformational differences between the two chain types, lends insight into the friction differences.

## Introduction

Self-assembled monolayers (SAMs) provide a flexible, convenient, and simple system with which to tailor the interfacial properties of metals, metal oxides, and semiconductors.<sup>1</sup> In addition, SAMs are promising candidates as boundary-layer lubricants for use in nanoscale devices.<sup>2–4</sup> They represent model systems for the study of lubrication at the molecular level because they can be formed under controlled conditions and form ordered, well-packed monolayers.<sup>4,5</sup> As a result, the frictional properties of SAMs have been studied extensively using atomic force microscopy (AFM).<sup>5–21</sup> The effects of chain length, packing density (order), and terminal group on friction are some of the variables that have been examined.

The alkyl chains of SAMs composed of *n*-alkanethiols on Au (111) are in the all-trans conformation and have a tilt of approximately 30° with respect to the surface normal.<sup>1,3</sup> As a consequence of this tilt angle, the orientation of the terminal methyl group in chains composed of an even number of methylene ( $-\text{CH}_2-$ ) units differs from those with chains composed of an odd number of methylene units. Sum frequency generation spectroscopy has been used to determine that the methyl angle, or the angle between the terminal carbon-carbon (C-C) bond and the surface normal, is 27° and 58° for chains with an odd and even number of methylene units, respectively.<sup>22</sup> This is known as the “odd-even” effect.

\* To whom correspondence should be addressed. E-mail: mikulski@usna.edu (P.T.M.); jah@usna.edu (J.A.H.).

† Department of Physics.

‡ Department of Chemistry.

§ Midshipman First-class.

(1) Love, J. C. E. L. A.; Kriebel, J. K.; Nuzzo, R. G.; Whitesides, G. M. Self-Assembled Monolayers of Thiolates on Metals as a Form of Nanotechnology. *Chem. Rev.* **2005**, *105*.

(2) Ashurst, W. R.; Yau, C.; Carraro, C.; Maboudian, R.; Dugger, M. T. Dichlorodimethylsilane as an anti-stiction monolayer for MEMS: A comparison to the octadecyltrichlorosilane self-assembled monolayer. *J. Microelectromech. Syst.* **2001**, *10*, 41–49.

(3) Ulman, A. Formation and Structure of Self-Assembled Monolayers. *Chem. Rev.* **1996**, *96*, 1533–1554.

(4) Dugger, M. T.; Senft, D. C.; Nelson, G. C. Friction and Durability of Chemisorbed Organic Lubricants for MEMS. In *Microstructure and Tribology of Polymer Surfaces*; Tsukruk, V. V., Wahl, K. J., Eds.; American Chemical Society: Washington, DC, 1999; pp 455–473.

(5) Salmeron, M. Generation of defects in model lubricant monolayers and their contribution to energy dissipation in friction. *Tribol. Lett.* **2001**, *10*, 69–79.

(6) Brewer, N. M.; Beake, B. D.; Leggett, G. J. Friction Force Microscopy of Self-Assembled Monolayers: Influence of Adsorbate Alkyl Chain Length, Terminal Group Chemistry, and Scan Velocity. *Langmuir* **2001**, *17*, 1970–1974.

(7) van der Vegte, E. W.; Subbotin, A.; Hadziioannou, G.; Ashton, P. R.; Preece, J. A. Nanotribological Properties of Unsymmetrical *n*-Dialkyl Sulfide Monolayers on Gold: Effect of Chain Length on Adhesion, Friction, and Imaging. *Langmuir* **2000**, *16*, 3249–3256.

(8) Carpick, R. W.; Salmeron, M. Scratching the Surface: Fundamental Investigations of Tribology with Atomic Force Microscopy. *Chem. Rev.* **1997**, *97*, 1163–1194.

(9) Kiely, J. D.; Houston, J. E. Contact Hysteresis and Friction of Alkanethiol Self-Assembled Monolayers on Gold. *Langmuir* **1999**, *15*, 4513–4519.

(10) Kim, H. I.; Koini, T.; Lee, T. R.; Perry, S. S. Systematic Studies of the Frictional Properties of Fluorinated Monolayers with Atomic Force Microscopy: Comparison of  $\text{CF}_3-$  and  $\text{CH}_3-$ Terminated Films. *Langmuir* **1997**, *13*, 7192–7196.

(11) Kim, H. I.; Graupe, M.; Oloba, O.; Doini, T.; Imaduddin, S.; Lee, T. R.; Perry, S. S. Molecularly Specific Studies of the Frictional Properties of Monolayer Films: A Systematic Comparison of  $\text{CF}_3-$ ,  $(\text{CH}_3)_2\text{CH}-$ , and  $\text{CH}_3-$ Terminated Films. *Langmuir* **1999**, *15*, 3179–3185.

(12) Leggett, G. J. Friction Force Microscopy of Self-Assembled Monolayers: Probing Molecular Organization at the Nanometer Scale. *Anal. Chim. Acta* **2003**, *479*, 17–38.

(13) Lee, S.; Shon, Y.-S.; Colorado, R.; Guenard, R. L.; Lee, T. R.; Perry, S. S. The Influence of Packing Densities and Surface Order on the Frictional Properties of Alkanethiol Self-Assembled Monolayers (SAMs). *Langmuir* **2000**, *16*, 2220–2224.

(14) Lee, S.; Puck, A.; Graupe, M.; Colorado, R., Jr.; Shon, Y.-S.; Lee, T. R.; Perry, S. S. Structure, Wettability, and Frictional Properties of Phenyl-Terminated Self-Assembled Monolayers on Gold. *Langmuir* **2001**, *17*, 7364–7370.

(15) Liley, M.; Gourdon, D.; Stamou, D.; Meseth, U.; Fischer, T. M.; Lautz, C.; Stahlberg, H.; Vogel, H.; Burnham, N. A.; Duschl, C. Friction anisotropy and asymmetry of a compliant monolayer induced by a small molecular tilt. *Science* **1998**, *280*, 273–275.

(16) Li, S. C. P.; Colorado, R., Jr.; Yan, X.; Wenzl, I.; Shmakova, O. E.; Graupe, M.; Lee, T. R.; Perry, S. S. Local Packing Environment Strongly Influences the Frictional Properties of Mixed  $\text{CH}_3-$  and  $\text{CF}_3-$ Terminated Alkanethiol SAMs on Au(111). *Langmuir* **2005**, *21*, 933–936.

(17) Lio, A.; Morant, C.; Ogletree, D. F.; Salmeron, M. Atomic Force Microscopy Study of the Pressure-Dependent Structural and Frictional Properties of *n*-Alkanethiols on Gold. *J. Phys. Chem. B* **1997**, *101*, 4767–4773.

(18) Perry, S. S.; Lee, S.; Shon, Y.-S.; Colorado, R., Jr.; Lee, T. R. The relationships between interfacial friction and the conformational order of organic thin films. *Tribol. Lett.* **2001**, *10*, 81–87.

(19) Shon, Y.-S.; Lee, S.; Colorado, R.; Perry, S. S.; Lee, T. R. Spiroalkanedithiol-Based (SAMs) Reveal Unique Insight into the Wettabilities and Frictional Properties of Organic Thin Films. *J. Am. Chem. Soc.* **2000**, *122*, 7556–7563.

(20) Wong, S.-S.; Takano, H.; Porter, M. D. Mapping Orientation Differences of Terminal Functional Groups by Friction Force Microscopy. *Anal. Chem.* **1998**, *70*, 5200–5212.

(21) Xiao, X.; Hu, J.; Charych, D. H.; Salmeron, M. Chain Length Dependence of the Frictional Properties of Alkylsilane Molecules Self-Assembled on Mica Studied by Atomic Force Microscopy. *Langmuir* **1996**, *12*, 235–237.

Many interesting phenomena associated with the odd–even effect have been observed. Shock waves were recently used to compress monolayers with odd and even numbers of methylene units.<sup>23</sup> Vibrational sum-frequency generation spectroscopy was used to probe the orientation of the terminal methyl groups. For monolayers in the all-trans conformation with an even number of methylene units, increasing the compression increased the methyl tilt. Unloading caused a return to the original tilt angle. In contrast, for chains with an odd number of methylene units, smaller degrees of compression resulted in the formation of terminal gauche defects. An odd–even effect has also been observed for chiral alkyl alcohols in solution using vibrational circular dichroism spectroscopy.<sup>24</sup>

Porter and co-workers used friction force microscopy to examine the friction of samples of SAMs that were composed of domains of pure *n*-alkanethiols that differed by one methylene unit.<sup>20</sup> Domains with an even number of  $-\text{CH}_2-$  units consistently yielded higher friction than those with an odd number of  $-\text{CH}_2-$  units, when the number of  $-\text{CH}_2-$  units is between 12 and 16. The friction of straight-chain alkanethiols terminated by phenyl groups ( $-\text{C}_6\text{H}_5$ ) was examined using AFM.<sup>14</sup> In that work, the authors concluded that no evidence of an odd–even fluctuation in friction was observed. In contrast to the findings of Porter and co-workers, Perry and co-workers recently observed no difference in friction for monolayers composed of  $\text{CH}_3(\text{CH}_2)_{14}\text{SH}$  chains compared to those composed of  $\text{CH}_3(\text{CH}_2)_{15}\text{SH}$  chains.<sup>16</sup>

Motivated by the aforementioned experimental work that has examined odd–even effects in SAMs, molecular dynamics (MD) simulations were used to compare the friction of *n*-alkane monolayers composed of an even number of carbon atoms (even monolayer) to those with an odd number of carbon atoms (odd monolayer). The chains are chemically bound to a diamond substrate, and an amorphous hydrocarbon tip is used to probe friction between the monolayers and the tip. This study focuses on the contact forces at the interface between the tip and individual monolayer atoms. The friction difference between the odd and even monolayers is elucidated by examining the distribution of contact forces, as well as the evolution of conformational changes, on interface atoms during sliding. The focus on individual chain groups gives insight to the nature of forces exerted on individual chain atoms over length scales of only a few angstroms, and thus provides a window into fundamental processes that is currently unavailable experimentally.

### Simulation Details

These simulations utilize a potential energy function that was parametrized to model hydrocarbon systems of all phases. The adaptive intermolecular reactive empirical bond-order potential (AIREBO), like the reactive empirical bond-order potential (REBO) from which it is derived, is capable of modeling chemical reactions.<sup>25</sup> Thus, the formation and creation of bonds that can accompany sliding are possible. Unlike REBO, AIREBO includes

long-range interactions between nonbonded atoms. While for most atomic pairs in the system it is very clear whether the atoms are bonded or not, during a chemical reaction, atomic pairs can arise for which the bonding characteristics are not clear. The strength of AIREBO is that it smoothly interpolates between the bound and unbound states in a self-consistent manner. This is accomplished by modifying simple pairwise interactions according to the local chemical environment of each pair. For instance, a pair separated by a distance greater than 2.0 Å will interact only through a pure Lennard–Jones (LJ) potential; however, at separations less than 2.0 Å, the local chemical environment of the pair is assessed to determine a factor between 0 and 1 which to some extent turns off the LJ interaction for this pair. This differentiates AIREBO from other reactive potentials, also based on REBO, that use only distance-based switching functions.<sup>26</sup> AIREBO has been used in earlier studies to model SAMs,<sup>27–34</sup> the compressibility of filled and unfilled nanotubes,<sup>35,36</sup> and the thermal conductivity of nanotubes.<sup>37</sup>

The model SAMs examined here contain *n*-alkane chains covalently bonded in a  $(2 \times 2)$  arrangement on a diamond (111) substrate (Figure 1). This system is tightly packed with an area of 21.9 Å<sup>2</sup> per chain and has approximately the same packing density as *n*-alkanethiols on gold (111).<sup>38</sup> The diamond substrates are composed of three layers of carbon atoms each containing 400 atoms. The lowest diamond layer is held rigid; a thermostat is applied to the remaining two layers. This system size has been shown to capture system dynamics in MD simulations of the friction of alkylsilane monolayers<sup>39</sup> and alkane monolayers.<sup>27</sup> Periodic boundary conditions of approximately 50 and 44 Å are imposed in the horizontal plane; the model systems are thus of an infinite tip and SAM (as opposed to a finite domain SAM). Two monolayers with 100 chains each were examined: an odd monolayer composed of 13 carbon-atom chains ( $-(\text{CH}_2)_{12}\text{CH}_3$ ), and an even monolayer composed of 14 carbon-atom chains ( $-(\text{CH}_2)_{13}\text{CH}_3$ ). The monolayer systems were equilibrated prior to combining with the model tip. Equilibration of the monolayers

(26) Che, J. C.; Cagin, T.; Goddard, W. A., III. Generalized extended empirical bond-order dependent force fields including nonbond interactions. *Theor. Chem. Acc.* **1999**, *102*, 346–354.

(27) Mikulski, P. T.; Gao, G.-T.; Chateauf, G. M.; Harrison, J. A. Contact Forces at the Sliding Interface: Mixed vs Pure Model Alkane Monolayers. *J. Chem. Phys.* **2005**, *122*, 024701-1–024701-9.

(28) Mikulski, P. T.; Harrison, J. A. Periodicities in the Properties Associated with the Friction of Model Self-Assembled Monolayers. *Tribol. Lett.* **2001**, *10*, 29–38.

(29) Mikulski, P. T.; Harrison, J. A. Packing-Density Effects on the Friction of *n*-Alkane Monolayers. *J. Am. Chem. Soc.* **2001**, *123*, 6873–6881.

(30) Chateauf, G. M.; Mikulski, P. T.; Gao, G. T.; Harrison, J. A. Compression- and Shear-Induced Polymerization in Model Diacetylene-Containing Monolayers. *J. Phys. Chem. B* **2004**, *108*, 16626–16635.

(31) Tutein, A. B.; Stuart, S. J.; Harrison, J. A. Role of Defects in the Compression and Friction of Anchored Hydrocarbon Chains on Diamond. *Langmuir* **2000**, *16*, 291–296.

(32) Tutein, A. B.; Stuart, S. J.; Harrison, J. A. Indentation Analysis of Linear-Chain Hydrocarbon Monolayers Anchored to Diamond. *J. Phys. Chem. B* **1999**, *103*, 11357–11365.

(33) Harrison, J. A.; Mikulski, P. T.; Stuart, S. J.; Tutein, A. B. *Nanotribology: Critical Assessment and Research Needs*; Hsu, S. M., Ying, Z. C., Eds.; Kluwer Academic Publishers: Norwell, MA, 2003.

(34) Harrison, J. A.; Stuart, S. J.; Tutein, A. B. A New, Reactive Potential Energy Function to Study the Indentation and Friction of C13 *n*-Alkane Monolayers. In *ACS Symposium Series: Interfacial Properties on the Submicron Scale*; Frommer, J., Overney, R. M., Eds.; American Chemical Society: Washington, DC, 2001; pp 216–299.

(35) Ni, B.; Sinnott, S. B.; Mikulski, P. T.; Harrison, J. A. Compression of Carbon Nanotubes Filled with C, CH<sub>4</sub>, or Ne: Predictions from Molecular Dynamics Simulations. *Phys. Rev. Lett.* **2002**, *88*, 205505-1–205505-4.

(36) Trotter, H.; Phillips, R.; Ni, B.; Hu, Y. H.; Sinnott, S. B.; Mikulski, P. T.; Harrison, J. A. Effect of filling on the compressibility of carbon nanotubes: Predictions from molecular dynamics simulations. *J. Nanosci. Nanotechnol.* **2005**, *5*, 536–541.

(37) Grujicic, M.; Cao, G.; Roy, W. N. Computational analysis of the lattice contribution to thermal conductivity of single-walled carbon nanotubes. *J. Mater. Sci.* **2005**, *40*, 1943–1952.

(38) Fenter, P.; Eberhardt, A.; Eisenberger, P. Self-Assembly of *n*-Alkyl Thiols as Disulfides on Au(111). *Science* **1994**, *266*, 1216.

(39) Chandross, M.; Grest, G. S.; Stevens, M. J. Friction between Alkylsilane Monolayers: Molecular Simulation of Ordered Monolayers. *Langmuir* **2002**, *18*, 8392–8399.

(22) Nishi, N.; Hobara, D.; Yamamoto, M.; Kakiuchi, T. Chain-length-dependent change in the structure of self-assembled monolayers of *n*-alkanethiols on Au(111) probed by broad-bandwidth sum frequency generation spectroscopy. *J. Chem. Phys.* **2003**, *118*, 1904–1911.

(23) Patterson, J. E.; Lagutchev, A.; Huang, W.; Dlott, D. D. Ultrafast Dynamics of Shock Compression of Molecular Monolayers. *Phys. Rev. Lett.* **2005**, *94*, 015501.

(24) Izumi, H. Y. S.; Futamura, S.; Nafie, L. A.; Dukor, R. K. Direct Observation of Odd–Even Effect for Chiral Alkyl Alcohols in Solution Using Vibrational Circular Dichroism Spectroscopy. *J. Am. Chem. Soc.* **2004**, *126*, 194–198.

(25) Stuart, S. J.; Tutein, A. B.; Harrison, J. A. A Reactive Potential for Hydrocarbons with Intermolecular Interactions. *J. Chem. Phys.* **2000**, *112*, 6472–6486.

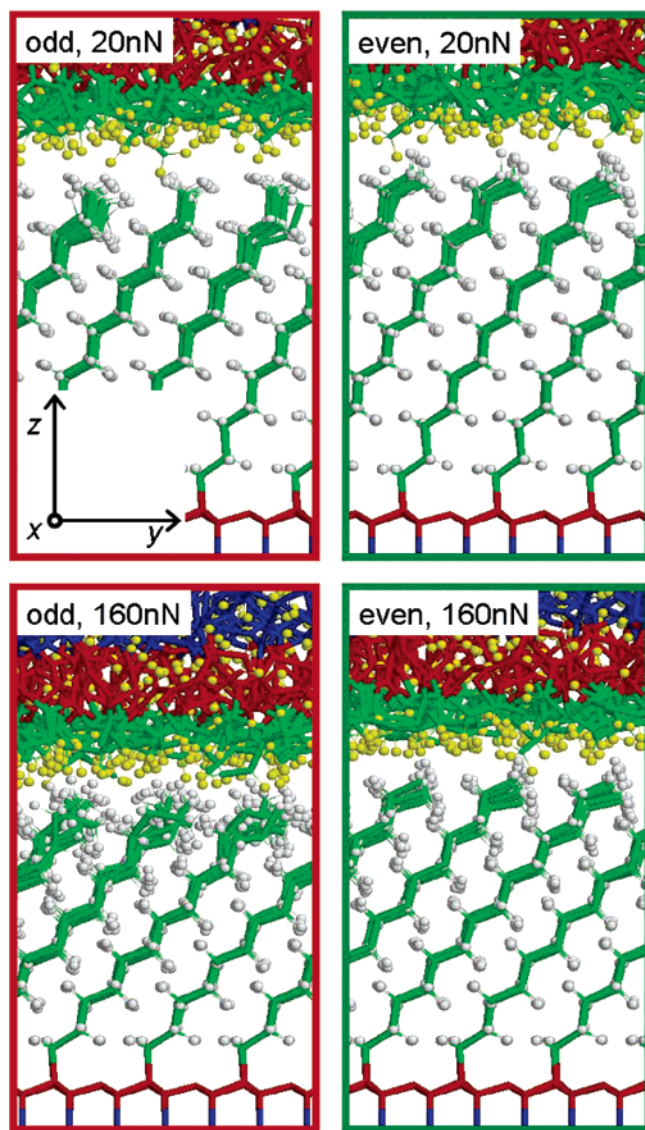


**Figure 1.** Snapshots of the model systems under investigation (monolayer type, load). Atoms in the blue and red regions are held rigid and thermostated, respectively. Wireframe format represents carbon atoms. Hydrogen atoms of the monolayers and tip are white and yellow, respectively. Sliding is in the positive  $y$  direction.

yields structures with chains canted predominantly in the positive  $y$  direction (Figure 1), as seen in previous simulations.<sup>27,29,31,32</sup>

The amorphous tip used here is that used in a related study<sup>27</sup> except that it has been reduced to nearly half its original thickness. The reduced thickness has no effect on the sliding dynamics. Of the 2803 atoms that make up the tip, the top 898 atoms are held rigid followed by 856 atoms that have a thermostat applied to them. The tip has a density of 2.3 g/cm<sup>3</sup> and contains 35% hydrogen; all bonds on the surface of the tip are saturated. The tip was constructed from amorphous carbon because a number of groups that perform AFM experiments of friction are beginning to use diamond-like carbon (DLC)-coated tips and because it is incommensurate with the monolayer. Several techniques for generating amorphous carbon samples have been described in the literature.<sup>40–50</sup> While the simple, effective, and most computationally feasible technique is the quenching of liquid carbon, it is difficult to generate amorphous carbon films with suitable surface structures using these methods,<sup>41,44</sup> ac-

ordingly, adaptations were made to the quenching techniques described in the literature and are described elsewhere.<sup>27</sup>

Sliding is simulated by moving the rigid atoms of the tip (blue in Figure 1) at a constant speed of approximately 0.22 Å/ps in the direction of chain cant (Figure 1). This speed is typical for MD simulations of this scale due to computational limitations<sup>27–32,39,51–54</sup> but orders of magnitude larger than experimental sliding speeds.<sup>8,10,11,20,55,56</sup> The effect of sliding speed on friction of alkylsilane monolayers<sup>39,51</sup> and diamond (100) surfaces<sup>57</sup> has been examined using MD. In these studies, the results were invariant in the range of computationally feasible sliding speeds (0.2–100 m/s). In hydrocarbon systems, the simulation time step is governed by the fastest process modeled, or the vibration of hydrogen atoms. With a time step of 0.20 fs, 2 million simulation steps were needed to travel two passes over the sample. This corresponds to a modeled sliding time of 400 ps and a sliding distance of 87 Å. Berendsen thermostats set at 290 K were applied separately to the tip and sample (red atoms in Figure 1) to dissipate the heat generated by sliding.<sup>58</sup> The results reported here are insensitive to the type thermostat used.

The sliding simulations reported here were conducted under constant loads from 20 to 320 nN in 20 nN increments. The load on the tip was maintained with a simple feedback loop in which the net loading force on the entire set of tip atoms exerted by the entire set of sample atoms was compared against a target load. All tip atoms were then accordingly moved up or down a fixed amount in addition to the usual molecular dynamics (further details are found in ref 27). The load range of 20–320 nN

(42) Gao, G. T.; Mikulski, P. T.; Harrison, J. A. Molecular-Scale Tribology of Amorphous Carbon Coatings: Effects of Film Thickness, Adhesion, and Long-Range Interactions. *J. Am. Chem. Soc.* **2002**, *124*, 7202–7209.

(43) Marks, N. A.; Cooper, N. C.; McKenzie, D. R. Comparison of density-functional, tight-binding, and empirical methods for the simulation of amorphous carbon. *Phys. Rev. B* **2002**, *65*, 075411-1–075411-9.

(44) Gao, G. T.; Mikulski, P. T.; Chateaufneuf, G. M.; Harrison, J. A. The Effects of Film Structure and Surface Hydrogen on the Properties of Amorphous Carbon Films. *J. Phys. Chem. B* **2003**, *107*, 11082–11090.

(45) Sinnott, S. B.; Colton, R. J.; White, C. T.; Shenderova, O. A.; Brenner, D. W.; Harrison, J. A. Atomistic simulations of the nanometer-scale indentation of amorphous-carbon thin films. *J. Vac. Sci. Technol. A* **1997**, *15*, 936–940.

(46) Kaukonen, H.-P.; Nieminen, R. M. Molecular-Dynamics Simulations of the Growth of Diamondlike Films by Energetic Carbon-Atom Beams. *Phys. Rev. Lett.* **1992**, *68*, 620–623.

(47) McCulloch, D. G.; McKenzie, D. R.; Goringe, C. M. Ab initio simulations of the structure of amorphous carbon. *Phys. Rev. B* **2000**, *61*, 2349–2355.

(48) Bilek, M. M. M.; McKenzie, D. R.; McCulloch, D. G.; Goringe, C. M. Ab initio simulation of structure in amorphous hydrogenated carbon. *Phys. Rev. B* **2000**, *62*, 3071–3077.

(49) Oleinik, I. I.; Pettifor, D. G.; Sutton, A. P.; Butler, J. E. Theoretical study of chemical reactions on CVD diamond surfaces. *Diamond Relat. Mater.* **2000**, *9*, 241–245.

(50) Jager, H. U.; Albe, K. Molecular-dynamics simulations of steady-state growth of ion-deposited tetrahedral amorphous carbon films. *J. Appl. Phys.* **2000**, *88*, 1129–1135.

(51) Park, B.; Chandross, M.; Stevens, M. J.; Grest, G. S. Chemical Effects on the Adhesion and Friction between Alkanethiol Monolayers: Molecular Dynamics Simulations. *Langmuir* **2003**, *19*, 9239–9245.

(52) Park, B. L. C. D.; Chandross, M.; Stevens, M. J.; Grest, G. S.; Borodin, O. A. Frictional Dynamics of Fluorine-Terminated Alkanethiol Self-Assembled Monolayers. *Langmuir* **2004**, *20*, 10007–10014.

(53) Tupper, K. J.; Colton, R. J.; Brenner, D. W. Simulations of Self-Assembled Monolayers under Compression: Effect of Surface Asperities. *Langmuir* **1994**, *10*, 2041–2043.

(54) Tupper, K. J.; Brenner, D. W. Compression-Induced Structural Transition in a Self-Assembled Monolayer. *Langmuir* **1994**, *10*, 2335–2338.

(55) Houston, J. E.; Kim, H. I. Adhesion, Friction, and Mechanical Properties of Functionalized Alkanethiol Self-assembled Monolayers. *Acc. Chem. Res.* **2002**, *35*, 547–553.

(56) Porter, M. D.; Bright, T. B.; Allara, D. L.; Chidsey, C. E. D. Spontaneously Organized Molecular Assemblies. 4. Structural Characterization of *n*-Alkyl Thiol Monolayers on Gold by Optical Ellipsometry, Infrared Spectroscopy, and Electrochemistry. *J. Am. Chem. Soc.* **1987**, *109*, 3559–3568.

(57) Perry, M. D.; Harrison, J. A. Universal Aspects of the Atomic-Scale Friction of Diamond Surfaces. *J. Phys. Chem.* **1995**, *99*, 9960–9965.

(58) Berendsen, H. J. C.; Postma, J. P. M.; van Gunsteren, W. F.; DiNola, A.; Haak, J. R. Molecular dynamics with coupling to an external bath. *J. Chem. Phys.* **1984**, *81*, 3684–3690.

(40) Marks, N. A.; McKenzie, D. R.; Pailthorpe, B. A.; Bernasconi, M.; Parrinello, M. Microscopic Structure of Tetrahedral Amorphous Carbon. *Phys. Rev. Lett.* **1996**, *76*, 768–771.

(41) Glosli, J. N.; Ree, F. H. Liquid–liquid-phase transformation in carbon. *Phys. Rev. Lett.* **1999**, *82*, 4659–4662.

corresponds to pressures of 0.90–14.4 GPa. The lower range of the target loads falls within the range routinely probed in AFM friction experiments.<sup>8,59,60</sup> Because of the periodic boundary conditions, high loads were required to examine chains with an increased cant in response to load. For chains in an isolated domain, such high loads may not be required to achieve similar cants though simulation of isolated domains is difficult due to the large number of atoms in the model systems.

Initial simulation configurations were created by placing the tip over the monolayers in positions that minimized the initial potential energy. Systems were then equilibrated while sliding along the direction of chain cant utilizing a target load of 20 nN. Once the systems showed steady-state dynamics, the system was adjusted to each of the target loads under continued sliding. Friction data were then collected for two passes across the sample for each system type under steady-state dynamics at each load (32 systems running in parallel). Two passes correspond to 10 unit cells as defined by the monolayer; a unit cell along the sliding direction is 8.71 Å.

## Results

Snapshots of the odd and even monolayers under 20 and 160 nN of load are shown in Figure 1. Under small repulsive loads, both monolayers are well ordered and have a uniform cant. However, the orientation of the terminal C–C bond is different in both monolayers. In the even monolayer, the C–C bond is significantly tilted away from the surface normal in the sliding direction, while it is nearly perpendicular to the diamond substrate in the odd monolayer. It should be noted that the orientation of the terminal C–C bond in the even monolayer corresponds to the orientation of the *n*-alkanethiol chains on Au discussed by Porter and co-workers<sup>20</sup> and by Nishi et al.<sup>22</sup> In those works, the odd–even designation corresponds to the number of methylene (–CH<sub>2</sub>–) units within a chain. Thus, both the sulfur atom which anchors the chain to the gold and the –CH<sub>3</sub> at the end of the chains are not included in the odd–even definition. In this work, the chains are anchored by a –CH<sub>2</sub>– group and terminated with a –CH<sub>3</sub>. The orientation of the terminal methyl group from the surface normal depends on the attachment group to the substrate and the identity of the substrate. For example, in contrast to *n*-alkanethiols on Au, the C–C bond is nearly perpendicular to the surface normal in chains with an even number of –CH<sub>2</sub>– units for *n*-alkanoic acid monolayers on Ag,<sup>61</sup> while the terminal methyl groups of chains with odd numbers of –CH<sub>2</sub>– units are tilted with respect to the surface normal.

In short, the main idea in contrasting “even” versus “odd” monolayers, however these terms are precisely defined, is to compare monolayers that are similar in structure with the exception of the orientation of the terminal bonds of chain backbones relative to the surface normal. In this study, the terminal C–C bonds of odd chains are oriented closer to the surface normal than the terminal C–C bonds of even chains which lie predominantly in the horizontal plane defined by the monolayer surface.

Increasing the load on the monolayer causes the chains within the even monolayer to increase their cant while

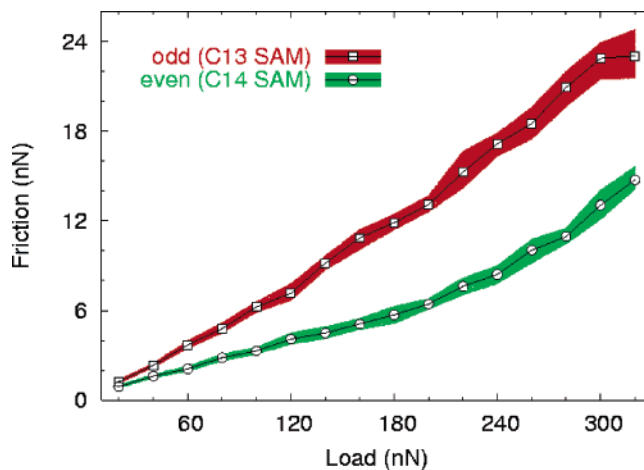


**Figure 2.** Friction as a function of load. The points correspond to the average friction taken over a series of unit cells. The shading indicates the standard deviation of unit-cell averages over the course of each slide. The same color coding is used in Figures 4, 5, 6, and 7.

maintaining their ordered structure at the sliding interface (lower panel, Figure 1). In contrast, the application of load to the odd monolayer introduces significant disorder into the monolayer at the sliding interface. These conformational differences between the odd and even monolayers significantly impact friction and will be discussed in detail later in this work.

Friction versus load data for the odd and even monolayers are shown in Figure 2. The points represent averages over the two passes across the sample. The shaded region indicates the standard deviations of the sets of unit-cell averages. The set for each system is constructed by calculating the friction for the first unit-cell window of the friction data set and then moving the window forward by one-hundredth of a unit cell and calculating again; this process is repeated until the two passes across the sample are covered. The full data set corresponds to 10 unit cells; thus, 901 possible unit cells comprise the set over which the standard deviation is assessed. Friction is calculated as the average force on the rigid atoms of the tip; because these atoms are moved with a constant velocity component along the sliding direction, we can directly connect this definition of friction with the rate at which energy associated with the friction force is deposited into the system (energy that is eventually removed by the atoms of the thermostats).

Over two passes across the sample, the odd monolayer always has higher friction than the even monolayer. For the odd monolayer, the friction versus load data is linear with a constant slope over the load range examined. In addition, as the load is increased, the standard deviation of unit-cell average friction values becomes wider (shaded region in Figure 2). In contrast, the friction versus load data for the even monolayer are linear; however, there is a change in slope at high loads ( $\sim 200$  nN). Such a change in slope has been recently observed by Houston and co-workers in the friction versus load behavior of –CH<sub>3</sub> terminated alkanethiol monolayers (interestingly, this change in slope was not evident in the –CF<sub>3</sub>-terminated alkanethiol monolayers in this comparative study).<sup>60</sup> Overall, the standard deviation of unit-cell average friction values is not as wide in the even monolayer compared to the odd monolayer.

In an effort to gain insight into the observed friction differences between the odd and even monolayers, the contact forces on the monolayers, the orientation of the

(59) Burns, A. R.; Houston, J. E.; Carpick, R. W.; Michalske, T. A. Friction and Molecular Deformation in the Tensile Regime. *Phys. Rev. Lett.* **1999**, *82*, 1181–1184.

(60) Houston, J. E.; Doelling, C. M.; Vanderlick, T. K.; Hu, Y.; Scoles, G.; Wenzl, I.; Lee, T. R. Comparative Study of the Adhesion, Friction, and Mechanical Properties of CF<sub>3</sub>- and CH<sub>3</sub>-terminated Alkanethiol Monolayers. *Langmuir* **2005**, *21*, 3926–3932.

(61) Tao, Y. T. Structural comparison of self-assembled monolayers of *n*-alkanoic acids on the surfaces of silver, copper, and aluminum. *J. Am. Chem. Soc.* **1993**, *115*, 4350–4358.

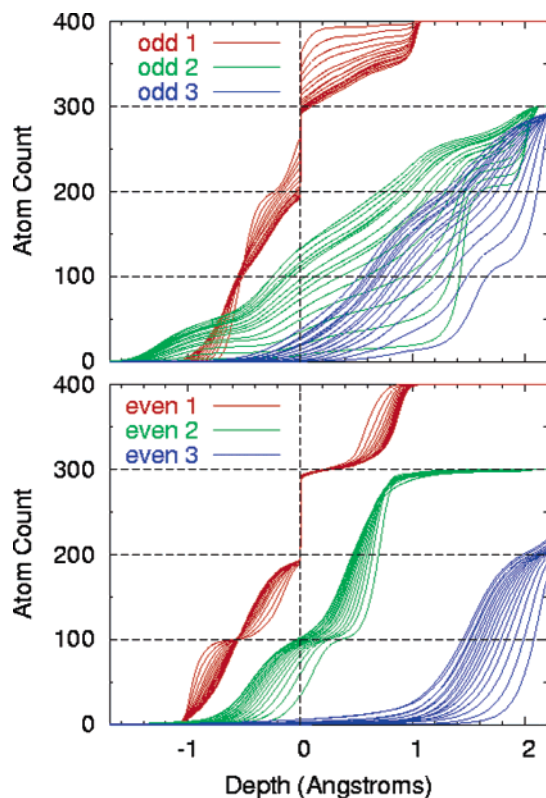


**Figure 3.** Integrated atom count as a function of monolayer depth. The carbon atom of each terminal methyl group ( $-\text{CH}_3$ ) is taken as local zero reference where negative/positive depths correspond to atoms above/below the reference terminal carbon atom. In the legend, the numbers 1 (red), 2 (green), and 3 (blue) refer to chain groups counting down the chain with 1 referring to the terminal group.

ends of the chains, and the rotation of the  $-\text{CH}_3$  group at the ends of the chains were examined. The integrated atom count of the top three groups in each chain versus monolayer depth is shown in Figure 3 for both monolayer types. The terminal carbon atom of each chain ( $-\text{CH}_3$ ) is taken to be depth zero and serves as a local reference for the top of the monolayer. Negative (positive) depths correspond to positions above (below) the terminal carbon atom. Progressing down the chain from the interface, each of the last three chain groups is represented by a color, red ( $-\text{CH}_3$ ), green ( $-\text{CH}_2-$ ), or blue ( $-\text{CH}_2-$ ). For each chain group, a series of lines (16 lines) is shown. Each line corresponds to a simulation at a different load.

Consider the  $-\text{CH}_3$  group of the even monolayer, the three “bulges” of the integrated atom count show the three hydrogen atoms of the terminal group in a structured arrangement that is maintained across the monolayer. Two hydrogen atoms are above the terminal carbon atoms and correspond to the “bulges” between  $-1.0$  and  $-0.5$  Å and  $-0.5$  and  $0.0$  Å in Figure 3. The instantaneous jump at zero depth accounts for the terminal carbon atoms. The third hydrogen atom is below the terminal carbon atom and corresponds to the “bulge” between  $0.5$  and  $1.0$  Å (Figure 3). Thus, the two hydrogen atoms above the terminal carbon atom are at slightly different heights with the remaining hydrogen atom buried deep below the terminal carbon atom. Progressing from low load to high load, the curves become more closely spaced. Thus, the initial application of load causes slight changes in height of the hydrogen atoms; however, there is a point where increasing the load does not change the height of the terminal hydrogen atoms significantly.

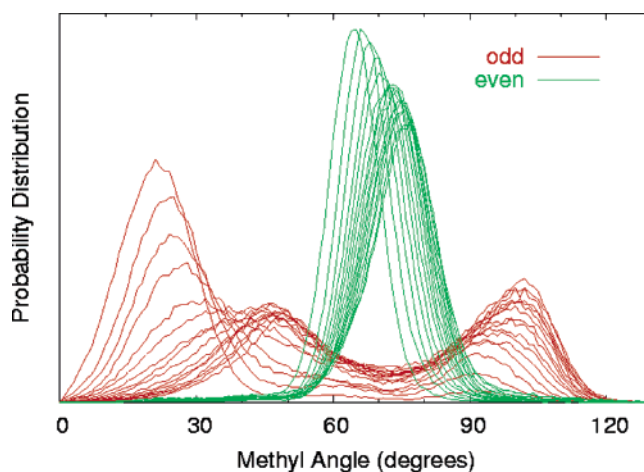


**Figure 4.** Probability distribution as a function of methyl angle. Color coding is the same as in Figure 2.

Moving into the even monolayer, the next chain group is a methylene group ( $-\text{CH}_2-$ ) and it is represented by the series of green lines in Figure 3. Again, the two “bulges” in this set of data correspond to the two hydrogen atoms and increasing the load causes the lines to be more closely spaced. Examination of the blue set of lines reveals that one hydrogen atom of the third  $-\text{CH}_2-$  group is typically within  $1.0$ – $2.0$  Å of the surface carbon atom.

The integrated atom count for the top three groups in chains from the odd monolayer is shown in the top panel of Figure 3. As before, the series of lines of a given color represents the different loads examined and more closely spaced lines within a color group represent moving to higher loads. In contrast to the even monolayer, the three hydrogen atoms from the terminal group are not localized to distinctly different depths. The lowest hydrogen atom hovers roughly around the same height as the parent carbon, while the other two occupy a region slightly above the parent carbon. The two higher hydrogen atoms, furthermore, are not as clearly distinguished, as evidenced by the lack of a plateau at an atom count of 100 (Figure 3). The lack of a hydrogen atom buried deep below the parent carbon is a key feature that distinguishes the odd monolayer from the even monolayer.

The second and third methylene groups show markedly different behavior than in the even monolayer. The hydrogen atoms of the second  $-\text{CH}_2-$  group are below the carbon atom of the terminal methyl group under low loads. This is also apparent in Figure 1. However, the application of load changes the conformation of the ends of the odd chains (Figure 1) such that the hydrogen atoms of the second  $-\text{CH}_2-$  group are above the terminal carbon atom and, at high enough loads, above even the terminal hydrogen atoms. While the hydrogen atoms of the third methylene group (blue lines) are far from the terminal carbon atom in the even monolayer, a significant number are close to the terminal group in the odd monolayer.

Conformational changes in the ends of the chains with the application of load can be further quantified by calculating the angle between the surface normal and the last C–C bond in each chain ( $-\text{CH}_2-\text{CH}_3$ ). This angle is known as the methyl angle and can also be obtained using sum-frequency vibrational spectroscopy.<sup>22</sup> Figure 4 shows the probability distribution of methyl angles for the odd and even monolayer. As in Figure 3, the series of lines of a given color represent the different loads examined and more closely spaced lines within a color group represent moving to higher loads. The probability distribution of methyl angles is calculated during the course of sliding

for all 100 chains in the systems. Under 20 nN of load, the distributions of both the odd and even monolayers are centered about one angle, with the angle being approximately twice as large for the even chains. It is worth noting that these methyl angles are very close to the experimentally determined values for *n*-alkanethiols on Au.<sup>22</sup>

For the even chains, increasing the load shifts the peak of the distribution to slightly larger angles and broadens it slightly. The largest changes in methyl angle occur before 100 nN with the degree of angle change slowing as the load is increased beyond 100 nN. This is manifest in Figure 4 by the green lines becoming successively more closely spaced and is also apparent from an examination of the percent volume change of the monolayer as a function of load (not shown). In contrast, the application of load to the odd monolayer causes a marked change in the methyl-angle distribution. The application of even a small amount of load results in the emergence of a peak near 100° (Figure 4). Thus, the final C–C bond in some of the chains is nearly parallel with the substrate. This peak corresponds to a terminal gauche conformation of the carbon backbone. A Newman projection of the second and third groups (viewing the spatial arrangement of hydrogen atoms while looking down the C–C bond that connects these groups) for a chain in such a gauche conformation reveals that a hydrogen atom from the second group lies between the two hydrogen atoms of the third group with each pair of hydrogen atoms on a given carbon atom spanning approximately 120°.

The additional application of load causes the structure of the distribution of the odd monolayer to continue to evolve with the peak in the methyl-angle distribution decreasing in intensity and shifting to larger angles. This is accompanied by the continued growth of the peak near 100°. Eventually, the methyl-angle distribution evolves into a bimodal distribution with broad peaks centered near 45° (no gauche defects in the carbon backbone) and 100° (gauche defects in the carbon backbone). Analysis of gauche defects shows that at the highest load over 60% of the chains are in the gauche conformation. In contrast, the number of gauche defects in the even monolayer is nearly constant (approximately 5%) over the load range examined.

Though friction calculated from the set of rigid atoms in the tip is closely connected with what is measured experimentally, it does not yield significant insight into interactions that occur at the sliding interface. A much more useful approach is to examine contact forces between the individual atoms of the monolayer and the full set of tip atoms. A contact friction could then be defined as the average of this force along the sliding direction summed over all monolayer atoms. The advantage of this approach is that the distribution of the atomic contact forces, the sum over which yields friction, gives useful information about what is going on at the sliding interface. There is no difference that can be discerned if the friction versus load plot of Figure 2 was constructed using this approach versus an analysis of rigid tip atoms only. While there can be much wider variations in instantaneous forces on the set of rigid atoms compared to the instantaneous contact forces on the entire set of monolayer atoms, the correlation between these two quantities is very tight. Consequently, we can proceed with a local analysis of contact forces with confidence. Such local analyses of contact forces have been utilized in previous MD simulations.<sup>27</sup>

Changes in the structure of the monolayers at the sliding interface markedly influence friction. Scaled friction and load values are shown as a function of total system load

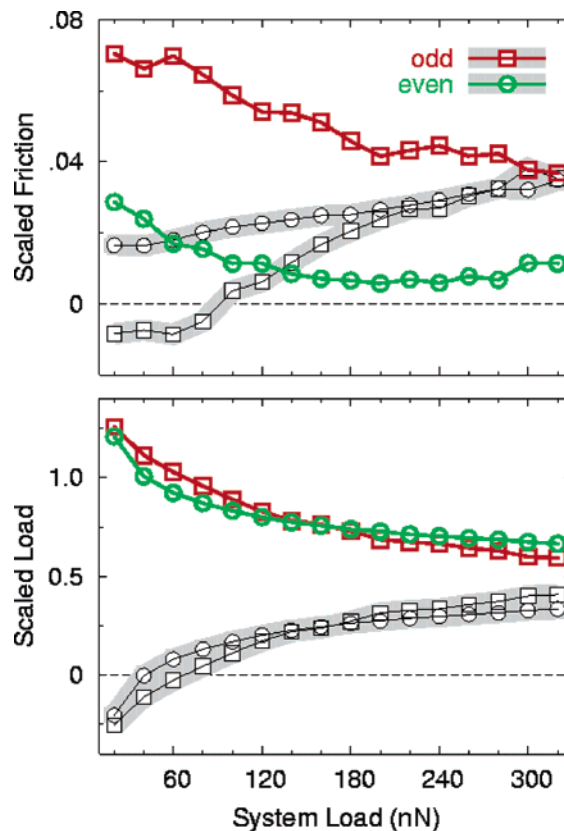


**Figure 5.** Scaled friction and scaled load as a function of system load. Green and red symbols correspond to terminal-group atoms ( $-\text{CH}_3$ ), and symbols in the gray-shaded regions correspond to atoms from nonterminal groups. Color coding is the same as in Figures 2 and 4.

in Figure 5 for both monolayers. In this plot, friction and load have been divided by the total system load to obtain scaled values. The scaled friction is broken into two components: the contact force in the sliding direction on the atoms from all terminal methyl chain groups ( $-\text{CH}_3$ ) (shown in color), and the contact force on the atoms from all nonterminal methylene chain groups ( $-\text{CH}_2-$ ) (gray shading). The second group in the chains, the methylene group just below the terminal group, is by far the dominant contributor to the friction shown in gray, though for the odd monolayer at the highest loads, the third group does contribute significantly. The scaled load is the sum of all the force components in the loading direction divided by the total system load.

It is clear from examination of the scaled load in Figure 5 that the bulk of the applied load is carried by the terminal groups for both the odd and even monolayers. At the lowest load of 20 nN, the groups below the terminal group are in attractive contact and thus the scaled load is  $>1$  for the terminal groups. As the system load is increased, the fraction carried by the terminal groups decreases rapidly (especially for the even monolayer) and, accordingly, the fraction carried by the nonterminal groups increases (the two fractions summed must give 1). Above a load of about 120 nN, the fraction of the load carried by the terminal groups continues to decrease though at a lower, approximately fixed rate.

The behavior of the scaled load for both the even and odd monolayers is similar over the entire load range examined. In contrast, the scaled friction for these two monolayers is quite different. For the scaled friction, the scaling factor is still the total system load; thus, there is no constraint on the sum of the scaled friction

from the terminal groups and the nonterminal groups (unlike for the scaled load for which this sum must be 1). The scaled friction of the terminal chain groups starts out high and decreases with the application of load for both the even and the odd chains. However, the friction of the terminal group in the odd monolayer is approximately twice that of the even monolayer. In addition, at loads lower than 100 nN, the friction contribution from the nonterminal groups is negative for the odd monolayer. This net “push” from the nonterminal groups may seem counterintuitive when thinking about friction; however, these groups are chemically bound to the terminal groups. Because bonding forces are much stronger than the nonbonded interactions between monolayer atoms and the tip, there is interplay between these terminal groups and the groups below (the net force summing atoms from all groups together is always “resisting”). As the load is increased over 100 nN, the nonterminal groups in the odd chains have a positive friction that grows in magnitude, but is always lower than the friction of the terminal group. At the highest loads, the terminal groups and the nonterminal groups contribute equally to the friction. The origin of this behavior lies in the conformational changes that take place in the monolayer as load is applied. Under low loads, the data shown in both Figures 1 and 3 demonstrate that only the terminal groups are in close proximity to the sliding interface. Thus, these groups are responsible for the bulk of the friction. As the load is increased, the atoms in the second (and third) groups come into close proximity with the sliding interface and, thus, are able to contribute significantly to the overall friction.

In the even monolayer at the lowest load, the contribution to the friction from the terminal chain groups is only slightly larger than the contribution from the nonterminal groups under low loads. As the load is increased, the contribution to friction from the nonterminal groups grows as the contribution from the terminal groups decreases. At the largest loads examined, the friction from the nonterminal groups is about 2.5 times larger than the contributions to friction from the terminal groups. As the load is increased, the atoms within the even monolayer become “locked” into position (fixed height in Figure 3), causing their contributions to the scaled friction to vary little as load is increased.

At any instant, the entire collection of tip atoms exerts a force on each atom in the monolayer. Taking the sliding direction as positive, a monolayer atom that experiences a positive force along the sliding direction from the tip is resisting the motion of the tip, negative indicates the atom is pushing the tip along. The average force on atoms while they are “resisting” can be tracked separately from the average force on atoms while they are “pushing”. If these forces are labeled  $F_R$  for “force resisting” and  $F_P$  for “force pushing”, friction can be broken down into the following form,

$$(\text{scaled friction}) = \frac{|F_R|}{(\text{system load})} \times \left( \frac{|F_R| - |F_P|}{|F_R|} \right)$$

The resisting force divided by the system load can be thought of as a force scale, the degree to which the monolayer is capable of generating forces along the sliding direction compared to the forces generated along the loading direction. This force scale is closely related to the roughness of the tip, the presence of tip asperities, and/or the roughness of the monolayer itself. Penetration into the monolayer would be associated with a large force scale, whereas compression of the monolayer would be associated

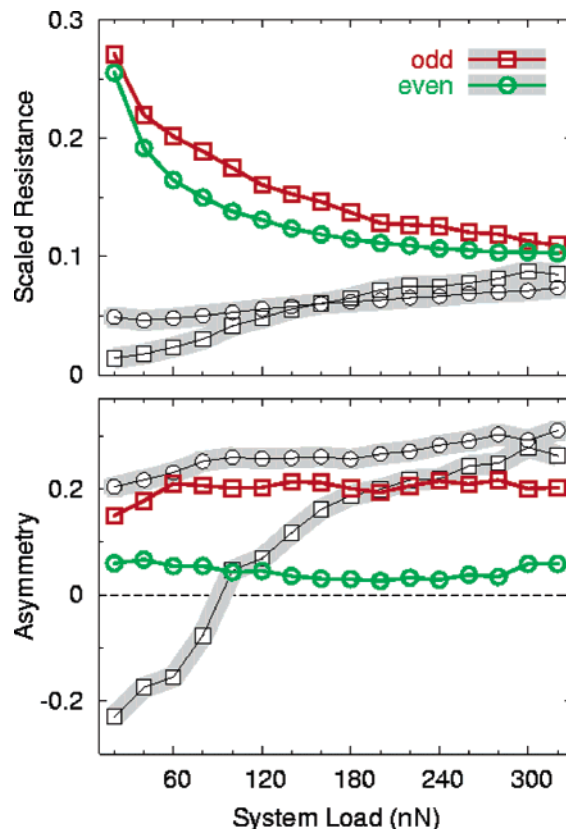


**Figure 6.** Asymmetry and scaled resistive force (positive) in the sliding direction as a function of total system load. Green and red symbols correspond to terminal-group atoms ( $-\text{CH}_3$ ), and symbols in the gray-shaded regions correspond to atoms from nonterminal groups ( $-\text{CH}_2-$ ).

with a small force scale. It is likely that the relative differences in friction between odd and even monolayers would disappear if a tip were utilized that delivered a significantly larger scaled resisting force. Evidence has been seen in recent simulations with rough tips.<sup>30,62</sup>

The factor  $((|F_R| - |F_P|)/|F_R|)$  in the above equation can be thought of as a measure of asymmetry where the upper limit value of +1 corresponds to a set of atoms that resist the motion of the tip but cannot respond with any pushing forces at all. An asymmetry of zero would mean no friction because pushing and resisting contributions are equal in size; negative asymmetry would indicate a pushing contribution that exceeds the resisting contribution. This breakdown of the friction is a local analysis of the dynamics at the sliding interface: the sign of the force on each individual atom at each data write must be determined in order to know whether to add it to the resisting-force sum or to the pushing-force sum with sums tracked separately for atoms belonging to a terminal chain group or a nonterminal chain group. Forces, which are written every 2000 simulation steps, are average forces exerted by the tip on each atom since the last data write.

The asymmetry and the scaled resisting force as a function of system load are shown in Figure 6 for both monolayers. Examination of the asymmetry of the even monolayer reveals that the asymmetry for terminal chain groups ( $-\text{CH}_3$ ) is smaller than it is for nonterminal chain groups. In addition to being very small overall, the asymmetry decreases as load is increased for low to moderate loads, is constant at moderate to high loads,

(62) Chateauneuf, G. M.; Van Workum, K.; Mikulski, P. T.; Gao, G. T.; Schall, J. D.; Harrison, J. A. *J. Phys. Chem. B*, in preparation.

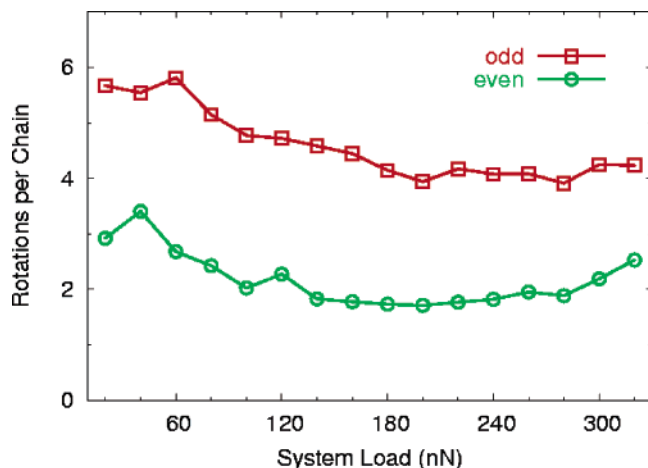


**Figure 7.** Rotations per chain of the methyl hydrogen atoms about the terminal C–C bond as a function of total system load. Color coding is the same as in Figures 2, 4, and 5.

and jumps a bit at the very highest loads. Roughly, the magnitude of the resisting and pushing forces,  $|F_R|$  and  $|F_P|$ , are nearly equal for the terminal groups of the even monolayer. In contrast, the asymmetry of nonterminal groups of the even monolayer is significant at all loads and shows a modest increase as the load is increased. These nonterminal groups, which for the even monolayer essentially means the second chain group, also exhibit a steadily rising scaled resistance which is directly connected with these groups taking on a higher fraction of the load as the load is increased. In short, for the even monolayer, the rise of the slope in the friction versus load curve reflects the increasing role of the nonterminal groups as the load is increased; the terminal groups maintain their nearly symmetrical force response along the sliding direction at all loads, though as the load is increased, they account for a decreasing fraction of the interface dynamics.

In contrast, the asymmetry of the terminal groups in the odd monolayer is significant at all loads. In addition, the atoms from nonterminal groups in the odd monolayer have the net effect of pushing on the tip for loads below 100 nN; however, the scale of forces associated with these atoms at these loads is very small and so this net effect of pushing is of little consequence. Above 100 nN, the asymmetry of the nonterminal groups becomes positive and increases to a value that is similar to the asymmetry of the nonterminal groups of the even monolayer. In this regime, these atoms bare a significant portion of the load and the friction, as seen in Figure 5. The scaled resistance versus load data (Figure 6) show that the odd and even monolayers resist tip motion similarly, though the terminal groups from the even monolayer exhibit a somewhat suppressed resisting force compared to those from the odd monolayer. It is the asymmetry that most dramatically distinguishes the terminal groups of the even monolayer compared to the odd.

In an effort to gain further insight into the way in which the geometry of the chains affects friction, the number of rotations that the terminal methyl group ( $-\text{CH}_3$ ) of each chain undergoes during sliding was plotted as a function of system load for both monolayers (Figure 7). The two C–C bonds from the last three groups in each chain ( $-\text{CH}_2-\text{CH}_2-\text{CH}_3$ ) are used to define a local coordinate system for each chain. The last C–C bond defines a local  $z'$  axis about which azimuthal angles are assessed, and the component of the next-to-last C–C bond that is perpendicular to the rotation axis defines a local  $x'$  axis which marks the zero azimuthal angle (the carbon atom

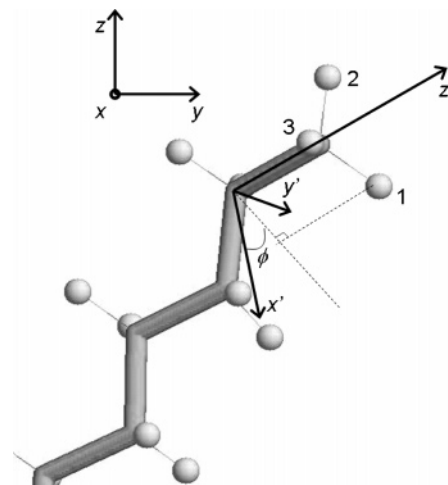


**Figure 8.** Azimuthal angle,  $\phi$ , of terminal hydrogen atom 1 defined in the chain's local coordinate system. The terminal C–C bond defines the  $z'$  axis, and the component of the second C–C bond perpendicular to the  $z'$  axis defines the  $x'$  axis;  $\phi$  lies in the  $x'y'$  plane.

just below the terminal carbon serves as an origin) (Figure 8). In this local coordinate system, the terminal hydrogen atoms appear locked in relative orientation with an approximate separation of  $120^\circ$  between the terminal carbon–hydrogen bonds projected into the chain's local  $x'y'$  plane. A rotation to a new conformation is a rotation through  $120^\circ$  to an equivalent geometry. The local coordinate system defined by the last three carbon atoms of a chain thus varies for each chain and for each instant in time. Instantaneous configurations are assessed every 2000 simulation steps. In general, the number of rotations decreases as the load is increased (Figure 7) for both monolayers; however, the number of rotations in the odd monolayer is almost twice that in the even monolayer.

Contact forces exerted by the tip on the three hydrogen atoms of terminal methyl groups as a function of azimuthal angle were also examined (Figure 9). While angles are assessed using instantaneous atomic coordinates every 2000 simulation steps, contact forces are average forces over these sets of 2000 simulation steps. To connect instantaneous angles with average contact forces, the angles at the start and finish of each 2000 simulation step interval are used to define a range where all angles in this range are weighted equally. Furthermore, the total weight for each interval is kept constant (a large change in angle means that the geometry spends less time near any of the angles in the interval). This treatment of angles is approximate because, in actuality, the angular velocity varies over the interval and angles can leave and re-enter the bounded region. In constructing the force distribution of Figure 9, the contact force on each terminal hydrogen atom over each 2000 simulation step interval is divided by the system's load, allowing all system loads to contribute to a single distribution function. The force distribution as a function of azimuthal angle for the even monolayer shows two sets of peaks. The peak around  $60^\circ$  is missing. Thus, the hydrogen atom that lies below its parent carbon atom is not contributing to the friction and it carries none of the applied load. The peak at  $180^\circ$  corresponds to the hydrogen atom that is at the highest distance above the monolayer (between  $-1.0$  and  $-0.5 \text{ \AA}$  in Figure 3), and the peak at  $320^\circ$  corresponds to the hydrogen atom that has a depth which is closest to the depth of the terminal carbon atom ( $0.0 \text{ \AA}$  in Figure 3). It is clear from these data that the top hydrogen atom ( $180^\circ$ ) carries a larger load than the other hydrogen atom. In addition, the magnitudes of the

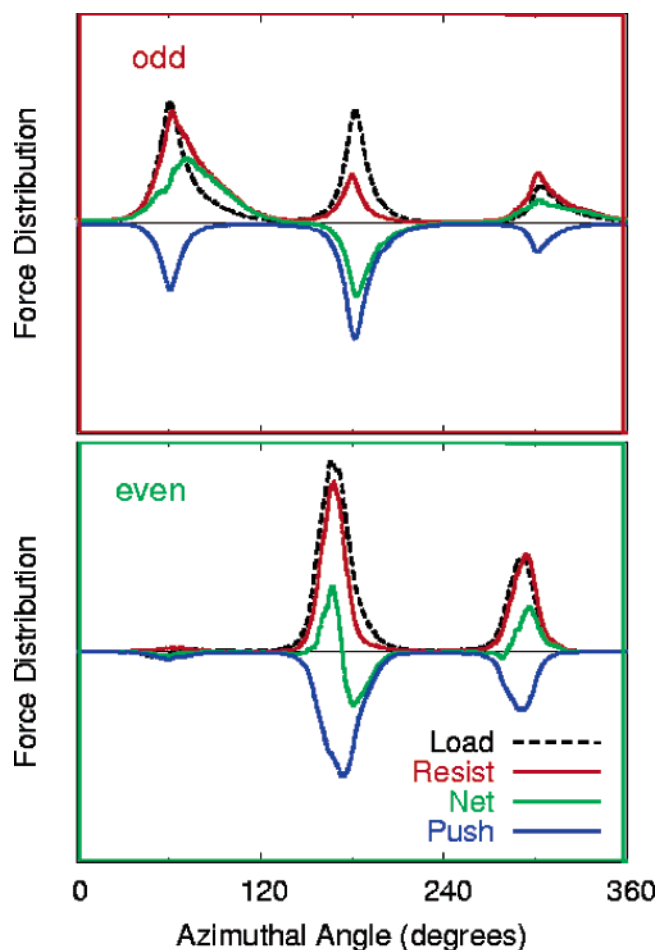


**Figure 9.** Contact force distributions for the three terminal hydrogen atoms of each chain as a function of azimuthal angle. Friction is the sum of the resisting and pushing contact forces.

resisting and pushing forces are larger than they are for the other hydrogen atom carrying a load. While it is not surprising that the hydrogen atom carrying the largest load also exhibits the largest resisting and pushing forces, it is surprising that the low asymmetry between resisting and pushing forces is associated primarily with this single hydrogen atom. In other words, this single hydrogen atom carries most of the load but contributes negligibly to the friction!

The orientation of terminal groups in the odd monolayer allows all three of the terminal hydrogen atoms to contribute to the contact forces in the sliding direction and to carry load. In this system, the peaks at  $60^\circ$  and  $180^\circ$  are the most interesting. These hydrogen atoms carry approximately equal portions of the system load. However, the hydrogen atom at  $60^\circ$  has large resistive forces and small pushing forces while the hydrogen atom at  $180^\circ$  has much small resistive forces and large pushing forces. The net pushing plus resistive forces as a function of angle (loosely thought of as the friction associated with an angle) shows interplay between two of the terminal hydrogen atoms in the odd monolayer by which one predominantly pushes while the other predominantly resists and the two taken together deliver significant friction. In contrast, a single terminal hydrogen atom from the even monolayer takes on both the dominant pushing and resistive roles and delivers negligible friction.

### Discussion

The structure of SAMs composed of *n*-alkanethiols on Au (111) that differ in length by one methylene unit

( $-\text{CH}_2-$ ) has been recently examined using broadband sum frequency generation spectroscopy.<sup>22</sup> In that work, it was determined that the orientation of the terminal methyl group differs for chains with even and odd numbers of  $-\text{CH}_2-$  units, with the angle between the terminal C–C bond and the surface normal for an even number of groups being almost twice as large as it is for an odd number of groups. This orientational difference, the “odd–even” effect, has been discussed in a number of recent papers.<sup>14,16,20,23,55,63,64</sup>

Several researchers have examined the friction of SAMs composed of alkanethiols that differed by one methylene unit. An odd–even effect in the friction was reported for samples patterned with alternating domains of *n*-alkanethiols, which was attributed to dipole-based differences in the surface free energies of the patterned regions.<sup>20</sup> However, it should be noted that recent AFM friction studies revealed no difference in the friction of *n*-alkanethiol SAMs composed of 15 carbon-atom chains compared to chains composed of 14 carbon-atom chains for loads between  $-20$  and  $20$  nN.<sup>16</sup>

The MD simulations detailed here aid in elucidating the aforementioned contradictory experimental findings. The simulations presented here show that the odd-chain SAMs have higher friction than the even-chain SAMs with the difference most pronounced when the load is sufficient enough to cause the chains to cant to a significantly higher degree than when not under load. At low loads in the odd monolayer, the terminal group of each chain is responsible for the bulk of the friction while both the terminal and second groups contribute substantially to the friction in the even monolayer. However, despite the fact that both the terminal and nonterminal groups contribute to the friction of even monolayer, its overall friction is comparable to the odd monolayer where the bulk of the friction comes solely from the terminal groups. It should also be noted, however, that these comments apply only to the friction generated by these groups and not to the load carried by these groups. These simulations clearly show that the magnitude of the load carried by the terminal group as a whole, for example, is approximately equal in the odd and even monolayers.

While the simulations presented here treat only SAMs composed of 14 carbon-atom chains and 13 carbon-atom chains, we expect the trends reported here to hold true generally for any well-packed even versus odd SAM. Experimentally, the fabrication of well-packed, ordered SAMs is only possible with chains longer than about 10 carbon atoms per chain, and the higher friction associated with short length chains is due to disorder brought about by the low packing density and disordered arrangement of chains on the substrate.<sup>21</sup>

The nature of MD simulations allows for the contact force distribution on the terminal groups of each chain to be analyzed on an atom-by-atom basis. Because the odd chains have a smaller methyl angle than the even chains under low loads, all three terminal hydrogen atoms have appreciable contact forces during sliding. In the odd monolayer, interplay exists between forces that resist and those that push tip motion. The magnitude of the resistive forces is significantly larger than the pushing forces on one hydrogen atom; the magnitudes are reversed on the second hydrogen atom and approximately equal on the third hydrogen atom. In contrast, only two hydrogen atoms of the terminal group have appreciable contact forces in the even monolayer with the scale of the forces being almost twice as large for one of the hydrogen atoms.

Increasing the load causes the friction of the odd and even monolayers to increase and causes changes in the

conformation of the monolayers. The load application causes a slight increase in the methyl angle of the chains in the even monolayer. The increase in methyl tilt occurs while the chains remain largely in their all-trans conformation as they do in shock compression studies.<sup>23</sup> The slight increase in the methyl angle is most pronounced between 0 and 100 nN. This results in a significant decrease in scaled friction for the terminal group and a slight increase in the scaled friction for the second group. It should be noted that the relative magnitudes of these contributions change as the load is applied. That is, the terminal group has slightly higher scaled friction than the second group at 20 nN, while at 100 nN the terminal has significantly lower scaled friction than the second group. The compression of the monolayer is responsible for this crossover. An examination of Figure 3 shows that compression pushes the hydrogen atoms from the second group closer to the interface and equalizes the depths of the highest two hydrogen atoms from the terminal group, while also burying the third hydrogen from the terminal group deeper into the monolayer.

The conformational changes that occur in the odd monolayer with the application of load are dramatic. The application causes significant increases in the methyl angles, which is consistent with recently reported shock compression results.<sup>23</sup> Salmeron and co-workers have also observed conformational changes in SAMs of OTS using sum-frequency generation.<sup>5</sup> As the load is increased, the chain groups below the terminal group gradually move closer to the surface as the terminal group is pushed down. Eventually, these groups move close enough to the surface (above 80 nN) to take on a repulsive load. As these groups take on a repulsive load, they make a transition from delivering a net “pushing” effect to a “resisting” one. Accordingly, as these groups become more substantial contributors to the overall friction, there is a drop in the scaled friction from the terminal group.

Friction implies dissipation of energy. In monolayer systems, there are a number of modes of energy dissipation available. One dissipation mode is the vibrational excitation of chemical bonds caused by sliding. As two sliding surfaces interact, the friction forces increase as the stress on these atoms increases (i.e., the surfaces “stick”). With continued sliding the atoms can “slip” past one another. When the slip occurs, chemical bonds at the interface are vibrationally excited. This vibrational excitation, or heat, is transferred to the rest of the contacting bodies and dissipates. This process has been quantified in previous MD simulations of contacting diamond surfaces.<sup>65</sup> The vibrational energy imparted to *n*-alkane monolayers composed of 13 carbon atoms by a rigid, infinitely flat counterface has also been previously examined using MD.<sup>28</sup> In that work, the vibrational energy of the monolayer as a function of the work done by the rigid flat counterface was shown to be linear. Because the counterface was rigid, the work was proportional to the friction. Because friction is approximately linear with load, vibrational excitation of the chains was found to be an

important mode of energy dissipation in monolayer systems. Analysis of the chain lengths during sliding also suggested that energy is transferred from the counterface to the monolayer via the stretching of the chains. This is also the case in the simulations presented here.

Another mode of energy dissipation is the energy associated with the changing bond angles which are associated with rotations about single bonds. For example, MD simulations that examined the friction of methyl-terminated diamond surfaces showed that the methyl group rotates about the C–C bond attaching it to the diamond surface in a turnstile manner.<sup>66</sup> Salmeron and co-workers suggested that the generation of terminal gauche defects at the surface of monolayer films may lead to a small amount of energy dissipation.<sup>5</sup> Previous work in our group utilized a flat counterface to examine the friction of monolayers composed of *n*-alkane chains and demonstrated that a small number of defects do form that are localized to the ends of the chains.<sup>29,31</sup> In this work, chains in each monolayer have some freedom to rotate about the terminal C–C bond. However, the freedom of the monolayer is different in the odd and even monolayers. In the even monolayer, chains are “locked” into conformations that allow for the symmetric response, or pushing, of the monolayer to resisting forces. One indication of a locked conformation is the single well-defined peak in the methyl-angle distribution of the even monolayer in contrast to the bimodal distribution of the odd monolayer (Figure 4). A second indication of the locked conformation is a suppression of rotations about the terminal C–C bond seen the even monolayer. It should be noted that these locked conformations are associated with steep potential energy barriers when sliding in the direction of chain cant. Changing the sliding direction leads to changes in the orientation of the chains as a whole and conformational changes within the chains. For instance, previous MD simulations of C<sub>14</sub> chains showed when sliding transverse to the chain cant, chains have a larger range of motion (and accordingly higher friction). Eventually, sliding in this direction led to a uniform realignment of the chains in the sliding direction.<sup>27</sup> Sliding against the chain cant leads to drastic conformational changes within the chains and a large degree of disorder within the monolayer (and thus higher friction).

In summary, the simulations presented here demonstrate that the friction of a tightly packed, odd monolayer is larger than an even monolayer when sliding in the direction of chain cant with the difference becoming more pronounced as the load is increased. Analysis of the contact forces between the tip and the chains allows for the elucidation of these differences in terms of conformational differences in the two systems. The simulations presented here make use of periodic boundary conditions to model a large monolayer without the influence of edge effects. Currently, larger scale studies are underway to examine the extent to which the general trends reported here are evident in finite-domain monolayers.

**Acknowledgment.** This work was supported by The Office of Naval Research (N00014-05-WX-20129) and The Air Force Office of Scientific Research (F1ATA04295G001 and F1ATA04295G002).

LA052044X

(63) Wenzl, I. Y. C. M.; Barriet, D.; Lee, T. R. Structure and Wettability of Methoxy-Terminated Self-Assembled Monolayers on Gold. *Langmuir* **2003**, *19*, 10217–10224.

(64) Chen, Y. C.; Zwolak, M.; Di Ventra, M. Inelastic effects on the transport properties of alkanethiols. *Nano Lett.* **2005**, *5*, 621–624.

(65) Harrison, J. A.; White, C. T.; Colton, R. J.; Brenner, D. W. Investigation of the Atomic-scale Friction and Energy Dissipation in Diamond using Molecular Dynamics. *Thin Solid Films* **1995**, *260*, 205–211.

(66) Harrison, J. A.; Colton, R. J.; White, C. T.; Brenner, D. W. Effect of atomic-scale roughness on friction: A molecular dynamics study of diamond surfaces. *Wear* **1993**, *168*, 127–133.